Electronic version of an article published as International Journal of Bifurcation and Chaos Vol. 17, No. 3, 2007, 985-998,
DOI: 10.1142/S0218127407017707 © World Scientific Publishing Company, https://www.worldscientific.com/worldscinet/ijbc

Bifurcations in Two-dimensional Hindmarsh-Rose Type Model

Shigeki Tsuji [†‡], Tetsushi Ueta [§], Hiroshi Kawakami [¶],
Hiroshi Fujii,[‖] and Kazuyuki Aihara [†‡]

We analyze a two-dimensional Hindmarsh-Rose type model exhibiting properties of both Class 1 and Class 2 neurons. Although the system is two-dimensional and contains only four parameters, the obtained bifurcation diagrams show that the bifurcation structure satisfies conditions for emergence of both features with constant stimuli.

Keywords: Neuronal excitability and spiking, Class 1 and Class 2 neurons, Hindmarsh-Rose model, FitzHugh-Nagumo model, Bifurcation theory

1 Introduction

Hodgkin suggested that there are two different classes of neurons, namely Class 1 and Class 2 neurons according to their frequency response characteristics when a constant current is injected to the cell body [Hodgkin, 1948]. Class 1 excitability is concerned with a saddle-node bifurcation in which the bifurcating state shows zero frequency response. On the other hand, Class 2 excitability is related to the Andronov-Hopf bifurcation, which is characterized by the fact that the bifurcating state holds a certain non-zero frequency. From the classification based on bifurcation theory, they have also been called Type 1 and Type 2, respectively [Rinzel & Ermentrout, 1989]. Many mathematical models have been proposed to describe neural activities [Izhikevich, 2000; Izhikevich, 2004], which may exhibit either or both of two firing modes.

Despite their high ability in the description of nerve dynamics, conventional high-dimension neuron models have potential degeneracy in bifurcations with high codimensions. Emergence of spikings is not always characterized by the Andronov-Hopf and saddle-node bifurcations in these models.

Notwithstanding of their simplicity, single neuron models reduced to two or three variable systems, such as the FitzHugh-Nagumo model (FHN) [FitzHugh, 1961; Nagumo *et al.*, 1962], the two- or three-dimensional Hindmarsh-Rose model [Hindmarsh & Rose, 1982; Hindmarsh & Rose, 1984; Rose & Hindmarsh, 1989], the Morris-Lecar model [Morris & Lecar, 1981], the Wilson model [Wilson, 1999], and the Izhikevich model [Izhikevich, 2004], may have advantages not only in their practicality in simulations with large scale coupled neuronal systems but also in its clarity of mathematical essence of bifurcation structure, i.e., the spike generation mechanism in terms of parameters. In fact, these models have been used to investigate the comparison of excitable properties and possible roles of these types in the cortical networks [St-Hilaire & Longtin, 2004; Tateno *et al.*, 2004].

[†]Aihara Complexity Modelling Project, ERATO, JST, 3-23-5-201 Uehara, Shibuya-ku, Tokyo 151-0064, Japan
[‡]Institute of Industrial Science, The University of Tokyo, 4-6-1 Komaba, Meguro-ku, Tokyo 153-8505, Japan
[§]Center for Advanced Information Technology, The University of Tokushima, 2-1 Minami-Josanjima, Tokushima 770-8506 Japan
[¶]The University of Tokushima, 2-24, Shinkura, Tokushima 770-8501, Japan
[‖]Department of Information and Communication Sciences, Kyoto Sangyo University, Kamigamo-Motoyama, Kita-ku, Kyoto 603-8555, Japan

In these reduced neuron models, although the FHN model is very popular, it shows only Class 2 excitability via the (subcritical) Andronov-Hopf bifurcation. Recently, it is reported [Fujii & Tsuda, 2004; Tsuda *et al.*, 2004] that two-variable Class 1^* neurons, defined as a subclass of Class 1, may exhibit an extensive spatio-temporal chaos when coupled by electrical synapses (gap junctions), while they exhibit only regular repetitive firings when isolated. This may show that the Class 1 excitability further reveals a new class of *system-level dynamics* which are not observed in Class 2 neurons, and show the significance of further mathematical studies. In this paper, we consider a two-dimensional Hindmarsh-Rose (2DHR) type model that retains the analytic tractability of the FHN model. Especially, to clarify what firing properties the 2DHR type model exhibits, we compute the bifurcation diagrams by changing some parameters in detail and examine the firing properties of this model.

2 Two-Dimensional Hindmarsh-Rose Type Model

Let us consider a reduced model of the following form:

$$\left\{ \begin{array}{rcl} \dfrac{dx}{dt} & = & f(x,y;z), \\ \dfrac{dy}{dt} & = & g(x,y), \end{array} \right. \tag{1}$$

where x and y denote the cell membrane potential and a recovery variable, respectively. z represents the external stimulus. The system may, in general, exhibit typical nonlinear phenomena such as the Andronov-Hopf and saddle-node bifurcations, separatrix loops, and hard oscillations depending on its nonlinearity and parameter values.

Specifically, the FHN model derived from the Hodgkin-Huxley model [Hodgkin & Huxley, 1952], takes the following form:

$$f(x,y;z) = c(x - x^3/3 - y + z), \quad g(x,y) = (x - by + a)/c. \tag{2}$$

The system of Eqs. (1) and (2) are characterized by the linearity of g, and consequently by Class 2 excitability and spiking [1)] for all the range of z.

In many neocortical neurons, however, it is known that membrane potential shows Class 1 excitability (see e.g., [Cauli *et al.*, 1997]). It is well recognized that Class1 excitability is, within the two-variable formulation, essentially characterized by the quadratic nonlinearity of the nullcline $g(x,y) = 0$. An example containing this characteristics is given by the 2DHR model [Rose & Hindmarsh, 1989] whose state variables are extracted from Connor's model [Connor *et al.*, 1977]. Note that Connor's model, actually derived from the Hodgkin-Huxley equations with an additional A-current component, preserves Class 1 excitability. Another example may be given by, though not intended to be a neocortical neuron model, the Morris-Lecar model with an appropriate parameter region [Morris & Lecar, 1981; Ermentrout, 1996; Govaerts & Sautois 2005; Tsumoto *et al*, 2006]. These systems show Class 1 excitability and spiking.

Motivated by these works, we introduce a generalized quadratic function into the FHN model (2), that is, $g(x,y) = 0$ is assumed as a parabolic nullcline. The equation is as follows:

$$f(x,y;z) = c\left(x - x^3/3 - y + z\right), \quad g(x,y) = (x^2 + dx - by + a)/c, \tag{3}$$

where d is a new parameter. Note that this model is equivalent to the 2DHR model (Eqs. (5) and (6) in [Hindmarsh & Rose, 1984]) if we consider the substitution of the state variable $y \mapsto -y$, and is also

[1)] Classification of "excitability" is characterized by the difference of bifurcation mechanism when the state of the system changes from an equilibrium or a small amplitude limit cycle to a large amplitude limit cycle by increasing the applied current. On the other hand, classification of "spiking" implies the difference of the frequency of terminating oscillations. Class 1 spiking system shows arbitrary low frequency and Class 2 spiking system shows a nonzero frequency, when the oscillation mode is terminated by decreasing the applied current (for detail, see Ref. [Izhikevich, 2000]).

a modification of Wilson's model of cortical neurons [Wilson, 1999]. Thus we call this model a 2DHR type model. In this letter, we analyze the dynamical behavior of Eqn. (3) with respect to the bifurcation structure.

3 Bifurcations in 2DHR Type Model

We assume hereafter $b = 1$, $c = 3$, and $z = 0$ that corresponds to a case without any external stimulus; the effect of non-zero z can be studied by the parameter a because changing the parameter a has the same effect for changing z, i.e., both parameters can translate the relative position of two nullclines, to the vertical direction in the state space. Therefore, without losing generality, we can investigate the bifurcation structure with $z = 0$.

Figure 1 shows a bifurcation diagram of limit sets of the solutions in Eqn. (3). In this figure, we follow the symbols defined in [Hoppensteadt & Izhikevich, 1997]. There exist the Andronov-Hopf (AH) and the saddle-node (SN) bifurcations for equilibria, where a superscription for SN may take 's' and 'u', which mean stable and unstable nodes, respectively. There also exists the saddle-node on limit cycle (SNLC) bifurcation in this system. As shown in an enlarged illustration in Fig. 1, many bifurcations including some high codimension bifurcations occur within a very small parameter range; there exist the Bogdanov-Takens (BT), the cusp (C) and the saddle-node on separatrix loop (SNSL) bifurcation points, and the saddle-separatrix loop (SSL) bifurcation curve. Two $\mathrm{SN^S}$ curves relevant to different equilibria are connected at the point C. Moreover, one is connected to AH, SSL, and $\mathrm{SN^u}$ curves in the point BT, and the other is connected to SSL and $\mathrm{SN^S}$LC curves in the point SNSL.

By these curves, Fig. 1 is divided into five topologically different regions as follows: Region (a) with a sink, Region (b) with a sink, a repeller, and a saddle, Region (c) with a repeller and a stable limit cycle, Region (d) with a sink, a repeller, a saddle, and a stable limit cycle, and Region (e) with two sinks and a saddle. Phase planes of these regions are shown in Fig. 2. As shown in Fig. 2, the periodic activity is obtained in a shaded area of Regions (c) and (d). A sink and a saddle that exist in Region (d) disappear by $\mathrm{SN^S}$ in Region (c). A small stable limit cycle exists just above the $\mathrm{SN^S}$ bifurcation, and moreover it exists in the very narrow area along the AH bifurcation curve. However, in this Region (c), it rapidly changes to a large limit cycle when the state of this system moves away from the AH bifurcation curve. This phenomenon is often called "*Canard*" [Eckhaus, 1983].

Observation of the dynamical behavior in Eqn. (3) with scanning a in the diagram of Fig. 1 for the fixed d means investigation of responses with various values of input stimulus z. Since there exist several bifurcation sets in the a-d parameter space, scanning a can meet different types of bifurcation sets with each value of d.

In the following, we show that both Class 1 and 2 excitability are possible in the dynamics of Eqn. (3). In Fig. 1, let us suppose that $d \lessapprox 2$, namely lower than the BT bifurcation point, and determine an appropriate value of a in Region (a). This fixed parameter values (a, d) is called here *an operating point*. The amplitude of an input z makes a left-right translation of this operating point in the diagram. Then the system (3) shows a Class 1 excitability and spiking feature by varying z. The essential reason why Class 1 excitability and spiking occur is the existence of the SNLC bifurcation curve that forms a border between Region (b) and Region (c). A perturbation of z equivalently makes a stride over this bifurcation set in the a-d parameter plane. Note that the $\mathrm{SN^u}$ curve between Region (a) and Region (b) is associated with an unstable node, thus it does nothing for excitability. Whereas, with fixing the parameter d at $d \gtrapprox 2$, a Class 2 excitability and spiking feature via the supercritical Andronov-Hopf bifurcation with "*Canard*" is observed by placing the operating point appropriately.

Next we illustrate a process causing Class 2 excitability and Class 1 spiking in Eqn. (3). Let us fix as $c = 3$ and $d = 1.8$. This parameter choice passes through $\mathrm{SN^S}$LC and $\mathrm{SN^u}$ bifurcation curves in Fig. 1 with a certain input z, i.e., the AH bifurcation does not happen in this case. The bifurcation structure in the a-b parameter plane is shown in Fig. 3. The diagram is divided into four regions. Each region has topologically different limit sets as follows: Region (a) with a stable equilibrium, Region (b) with

a sink, a repeller, and a saddle, Region (c) with a sink, a repeller, a saddle, and a stable limit cycle, and Region (d) with a repeller and a stable limit cycle. We show the phase portraits of these regions in Fig. 4. Regardless of initial conditions, a quiescent state is obtained in Regions (a) and (b) as shown in Fig. 4. Stable periodic spiking is observed in Region (d). There exists bistability in Region (c). It is noteworthy that the $\mathrm{SN^SLC}$ bifurcation curve is split into $\mathrm{SN^S}$ and SSL curves at the SNSL bifurcation point. Let us assume that $a \approx 0$ and b is less than the value causing the SNSL bifurcation. Then the corresponding operating point is located in Region (b). Thus the system behaves as a quiescent state without an input. As $z > 0$ increases, the operating point moves into Region (c) virtually, however, the state keeps quiescent since the SSL bifurcation does not affect the existing equilibrium point. With more increment of z, the operating point moves into Region (d). The stable equilibrium disappears by touching $\mathrm{SN^S}$, then we have spiking with a non-zero frequency value. This process results in Class 2 excitability. In the inverse process, since the spiking is not related with the saddle-node bifurcation of equilibrium points, the frequency of the spiking vanishes gradually as the operating point approaches the SSL curve. Finally the spiking is terminated and we have a quiescent state. Hence a Class 2 excitable and Class 1 spiking process is demonstrated.

Finally we show other possible bifurcations with $c = 3$ and $d = 2.2$ where the Class 2 oscillation is widely observed as shown in Fig. 5. The existence of the AH bifurcation generates the Class 2 oscillation with appropriate placing of the operating point. The SAH (subcritical Andronov-Hopf) and the DLC (double limit cycle) bifurcations form a narrow region (Region (c)) in the upper part of Fig. 5. As shown in Fig. 6, a stable equilibrium, a stable limit cycle, and an unstable limit cycle exist in Region (c), and hence a hard oscillation is possible in this model. While the dynamical behavior is almost the same as the Class 2 oscillation generated by the supercritical AH bifurcation except whether the bistable activity is shown or not, the Class 2 excitability and Class 1 spiking process with a hysteresis is observed in the lower part of Fig. 5. This is caused by SSL and SN^s bifurcation curves like Fig. 3.

Figure 7 shows relations between the firing frequency f and the input amplitude z. A wide range of the firing frequency and the zero frequency, which are typical properties of the Class 1 neuron, are confirmed by Fig. 7(a). In contrast, there exists a discontinuous jump caused by the supercritical AH bifurcation in Fig. 7(b). Figure 7(c) shows Class 2 excitability and Class 1 spiking with the bistability, while Fig. 7(d) shows Class 2 excitability and Class 2 spiking with the bistability [Izhikevich, 2000].

4 Concluding Remarks

The aim of this paper is to explore dynamical possibility of two-variable dynamical systems with essentially quadratic and cubic shapes of nullclines. Our results show the richness of dynamics and bifurcation structure which those systems may basically possess. This situation may become clear if we compare the bifurcation diagrams shown in this paper with those of, e.g., FHN model, a typical and well-established model for qualitative study of neuronal firings. It should be noted, however, that those models, including the FHN model, with an essentially *linear* nullcline instead of a quadratic one, were 'abstracted' from a particular class of neuronal systems, i.e., the Hodgkin-Huxley equations with sodium and potassium channels, and some ion channels properties are *a priori* excluded from the formulation. Our study presents a new perspective to dynamics of systems with a more general ion channels including the FHN system and others, viewed from a neuroscience standpoint.

What differentiates the excitability of a neuron into Class 1 and 2 is not a simple question within the framework of the Hodgkin-Huxley formulation with a large number of ion channels. However, within the reduced two-variable model of Eqs. (1) and (3), the key property which differentiates the two classes of excitability lies essentially in whether the two nullclines transversally cross each other or become tangent when a bifurcation parameter crosses a threshold value (or, at a critical point). Thus, it can happen that a small change of parameters may change the transversality of the two nullclines, and hence excitability of neurons. In fact, the bifurcation diagrams illustrate this possibility for the simple model with a quadratic recovery curve. In our reduced model composed of cubic and quadratic nullclines, this is in fact controlled

by the position of local minimum and the gradient of the second nullcline (i.e., $-d/2$, b respectively). Note that (a change of) the value d in our model could be regarded as (a change of) certain conductance variables (especially, the effect by changing an A-current) in the 2DHR model that is the reduced Connor model [Connor & McKown, 1977] (for details, see Eqn. (9) in [Rose & Hindmarsh, 1989]).

Our bifurcation diagrams show that there exist in principle four primary excitability and spiking properties, and as is shown in Fig. 7 they can be switched when one or two parameters are changed. In "Class 1 excitability and spiking" and "Class 2 excitability and spiking" systems without the bistability, the state changes between the rest state and repetitive firing only by the saddle-node on limit cycle bifurcation and the supercritical Andronov-Hopf bifurcation, respectively (e.g., see Fig. 1, and 7(a) and (b)). In "Class 2 excitability and Class 1 spiking", the state changes from the rest state to the repetitive firing by the saddle-node bifurcation (off limit cycle), and then the system shows a non-zero frequency. In contrast, the oscillation is terminated by the saddle-separatrix loop bifurcation, and then the system shows a zero frequency on the SSL bifurcation curve (e.g., see, Fig. 3, and 7(c).). Moreover, the system exhibits the bistability in the parameter region between these curves. Similarly, we can also obtain "Class 2 excitability and spiking" system with the bistability as shown in Fig. 7(d), and then the subcritical Andronov-Hopf bifurcation and the double limit cycle bifurcation are concerned with this mode (see, Fig. 5). Additionally, in Fig. 1, the existence of the Bogdanov-Takens (double-zero) bifurcation point, where the number of equilibrium and their stability change, is important to switch between both of two excitabilities.

As is mentioned in the above, a two-variable reduced model can be of both Class 1 and Class 2 depending on parameters. For instance, a shift of the rectifying potassium activation curve may make the corresponding reduced model to act as both Class 1 and Class 2 neurons. A possible origin of the quadratic(-like) nonlinearity of the second nullcline $\{(x, y)|g(x, y) = 0\}$ for the recovery variable is the introduction of A-currents, as is shown in the two-variable Hindmarsh and Rose model [Hindmarsh & Rose, 1982; Rose & Hindmarsh, 1989]. In fact, the latter was reduced from a six-variable Hodgkin-Huxley type equations with *additional* terms corresponding to 'an A-current' (Connor *et al.* [1977]). The resulting two-variable system could exhibit saddle-node bifurcations due to the quadratic-like nonlinearity if a parameter set is appropriately chosen. This appears to endorse Rogawski's experimental intuition [Rogawski, 1985] that the presence of "the" transient slowly inactivating potassium current I_{A} is the basis for the Class 1 excitability. However, it is worth noting that the Class 1 excitability, or more precisely, the quadratic nonlinearity in the two-variable model, is not necessarily a result of introduction of an A-current. An example is the Morris-Lecar model which shows both excitability depending on a form of the potassium activation curve [Ermentrout, 1996; Govaerts & Sautois 2005; Tsumoto *et al.*, 2006].

Hodgkin described in 1948 [Hodgkin, 1948] typical behaviors of Class 1 and 2 "neurons" (in fact, axons) as the strength of the applied current changes based on his experimental observations. Class 1 "axons are capable of repetitive firing over a wide range of frequencies, varied smoothly over a range of about 5-150 impulses per sec.", which is certainly a typical behavior of neurons with a saddle-node bifurcation. On the other hand, he wrote that Class 2 "axons usually give a train of impulses of frequency 75-150 /sec which was relatively insensitive to changes in the strength of the applied current". We note that although this insensitivity of frequency to changes of current strength may characterize the typical Andronov-Hopf bifurcations, and which is in fact the case for the FitzHugh-Nagumo model, the 2DHR-type model shows Class 2 excitability with, depending on its parameter range, a sharp increment of the firing frequency (see Fig. 7(b)). In this regard, it is worthy of noting that fast-spiking (FS) neurons in the neocortex exhibit such "specific" Class 2 excitability. That is, they have a low frequency firing (about 20[Hz]) near the spiking threshold and show a high sensitivity of the firing frequency on the applied current strength [Tateno et al., 2004]. A "typical" Class 2 excitability can emerge also in the 2DHR-type model if the second nullcline is made essentially linear in a certain range of the membrane potential by changing parameters (data not shown).

These results may suggest that some neurons can dynamically switch two excitabilities or can show mixed characteristics (e.g., a Class 2 oscillation with some characteristics of a Class 1 neuron) by

the shift of the (in)activation curve of a potassium channel or an A-current channel caused by the (de)phosphorylation of the channel protein [Chung et al., 1997; Mu et al., 2000]. In addition, an precise classification only by the difference of the bifurcation type may be difficult, if we consider a two-variable neuron model. In other words, small differences not identified in the classification of the bifurcation type may have a great influence on the system-level behavior. We might have to classify it in a consideration of other characteristics (e.g., the stability of an equilibrium inside a limit cycle, relative position and the shape of nullclines, etc.) [Fujii & Tsuda, 2004]. A detailed classification according to the bifurcation type is, on the other hand, also required [Govaerts & Sautois 2005].

Attention should be paid, however, to the limitation of two-variable reduced models. As is already mentioned, a reduced model is obtained from extended Hodgkin-Huxley-type equations after a series of reduction processes based on some *a priori* assumptions. Consequently, the correspondence between ion channel properties in HH equations and the nonlinearity in the reduced model is not one-to-one, but many-to-one. Moreover, the possibility can not be excluded in principle that certain dynamic properties in the original HH equations could be lost in the reduced model. Consequently the method presented here can not answer the following question (which is *an inverse problem*) directly: "what are the ion channel properties which *reproduce* the bifurcation structure realized in the reduced two-variable model?" However, despite the above problems, it is probable that there may exist some HH systems which can reproduce the rich nonlinear dynamics in the reduced systems at least up to some approximation. Whether such HH systems, or the obtained range of parameters, have reality should need a separate consideration from neuroscience standpoints.

Final remark is on the system-level behavior of neurons with Class 1 excitability. Recently, it is reported [Fujii & Tsuda, 2004; Tsuda *et al.*, 2004] that two-variable Class 1* neurons, defined as a subclass of Class 1, may exhibit an extensive spatio-temporal chaos when coupled by electrical synapses (gap junctions), while they exhibit only regular repetitive firings when isolated. Also the possibility is suggested that the chaotic dynamics are driven by a non-classical attractor in the sense of Milnor [1985]. It has not been reported that a similar dynamics could occur among a coupled system of Class 2 neurons. These findings suggest that the Class 1 excitability may further reveal a new class of *system-level dynamics* which are not observed in Class 2 neurons, and show the significance of further mathematical studies.

5 Acknowledgments

The authors would like to thank Dr. K. Tsumoto of Aihara Complexity Modelling Project, ERATO, JST for his helpful advice and fruitful discussion. This work was partly supported by the Advanced and Innovational Research Program in Life Sciences and by Grant-in-Aid for Scientific Research on Priority Areas 17022012 from the Ministry of Education, Culture, Sports, Science, and Technology, the Japanese Government.

References

[1] Cauli, B., Audinat, E., Lambolez, B., Angulo, M. C., Ropert, N., Tsuzuki, K., Hestrin, S. and Rossier, J. [1997] "Molecular and physiological diversity of cortical nonpyramidal cells," *J. Neurosci.*, **17** 3894–3906.

[2] Chung, I. & Schlichter, L. C. [1997] "Regulation of native Kv1.3 channels by cAMP-dependent protein phosphorylation," *Am. J. Physiol. Cell. Physiol.*, **273**, 622–633.

[3] Connor, J. A., Walter, D. & McKown, R. [1977] "Neural repetitive firing: modifications of the Hodgkin-Huxley axon suggested by experimental results from crustacean axons," *Biophys. J.* **18**, 81–102.

[4] Eckhaus, W. [1983] "Relaxation oscillations including a standard chase on French ducks," *Lect. Notes in Math.*, **985**, 449–494.

[5] Ermentrout, G. B. [1996] "Type I membranes, phase resetting curves and synchrony," *Neural Comput.*, **8**, 979–1001.

[6] FitzHugh, R. [1961] "Impulses and physiological state in theoretical models of nerve membrane," *Biophy. J.* **1**, 445–467.

[7] Fujii, H., & Tsuda, I. [2004] "Itinerant Dynamics of Class I* Neurons Coupled by Gap Junctions," *Cortical Dynamics*, eds. Eŕdi, P., Esposito, A., Marinaro, M., and Scarpetta, S., Lecture Notes in Computer Science (Springer-Verlag), Vol.3146, 140–160.

[8] Govaerts, W. & Sautois, B. [2005] "The onset and extinction of neural spiking: a neumerical bifurcation approach," *J. Comput. Neurosci.*, **18**, 265–274.

[9] Hindmarsh, J. L. & Rose, R. M. [1982] "A model of the nerve impulse using two first-order differential equations," *Nature*, **296**, 162–164.

[10] Hindmarsh, J. L. & Rose, R. M. [1984] "A model of neuronal bursting using three coupled first order differential equations," *Philos. Trans. R. Soc. London*, *Ser.* **B221**, 87–102.

[11] Hodgkin, A. L. [1948] "The local electric changes associated with repetitive action in a non-medullated axon," *J. Physiol.* **107**, 165-181.

[12] Hodgkin, A. L. & Huxley, A. F. [1952] "A qualitative description of membrane current and its application to conduction and excitation in nerve," *J. Physiol.* **117**, 500–544.

[13] Hoppenstead, F. C. & Izhikevich, E. M. [1997] *Weakly Connected Neural Networks*, (Springer-Verlag, NY).

[14] Izhikevich, E. M. [2000] "Neural excitability, spiking and bursting," *International Journal of Bifurcation and Chaos*, **10**, 1171–1266.

[15] Izhikevich, E. M. [2004] "Which model to use for cortical spiking neurons?," *IEEE Transactions on Neural Networks*, **15**, 1063–1070.

[16] Milnor, J. [1985] "On the concept of attractor," *Communications in Mathematical Physics*, **99**, 177–195.

[17] Morris, C. & Lecar, H. [1981] "Voltage oscillations in the barnacle giant muscle fiber," *Biophys.* **35**, 193–213.

[18] Mu, J., Zhuang, S. Y., Hampson, R. E. & Deadwyler, S. A. [2000] "Protein kinase-dependent phosphorylation and cannabinoid receptor modulation of potassium A current ($I_{\rm A}$) in cultured rat hippocampal neurons," *Pflügers Arc. Eur. J. Physiol.*, **439**, 541–546.

[19] Nagumo, J., Arimoto, S. & Yoshizawa, S. [1962] "An active pulse transmission line simulating nerve axon," In *Pro. of IRE* **50**, 2061–2070.

[20] Rinzel, J. & Ermentrout, G. B. [1989] "Analysis of neural excitability and oscillations," eds. C. Koch, & I. Segev, *Methods in Neuronal Modeling* (The MIT Press, Cambridge).

[21] Rogawski, M. A. [1985] "The A-current: how ubiquitous a feature of excitable cells is it ?" *TINS.* **8**, 214–219.

[22] Rose, R. M. & Hindmarsh, J. L. [1989] "The assembly of ionic currents in a thalamic neuron I. The three-dimensional model," *Proc. R. Soc. Lond.* **B** 237, 267–288.

[23] St-Hilaire, M. & Longtin A. [2004] "Comparison of coding capabilities of Type I and Type II neurons," *J. Comput. Neurosci.* **16**, 299–313.

[24] Tateno, T., Harsch, A. and Robinson, H. P. C. [2004] "Threshold firing frequency-current relationships of neurons in rat somatosensory cortex: Type 1 and Type 2 dynamics," *J. Neurophysiol.* **92**, 2283–2294.

[25] Tsuda, I., Fujii, H., Tadokoro, S., Yasuoka, T., and Yamaguti, Y. [2004] "Chaotic Itinerancy as a Mechanism of Irregular Changes between Synchronization and Desynchronization in a Neural Network," *J. Integrative Neuroscience*, **3**, 159–182.

[26] Tsumoto, K., Kitajima, H., Yoshinaga, T., Aihara, K. and Kawakami, H. [2006] "Bifurcations in Morris-Lecar neuron model," *Neurocomputing*, **69**, 293–316.

[27] Wilson, H. R. [1999] "Simplified dynamics of human and mammalian neocortical neurons," *J. theor. Biol.* **200**, 375–388.

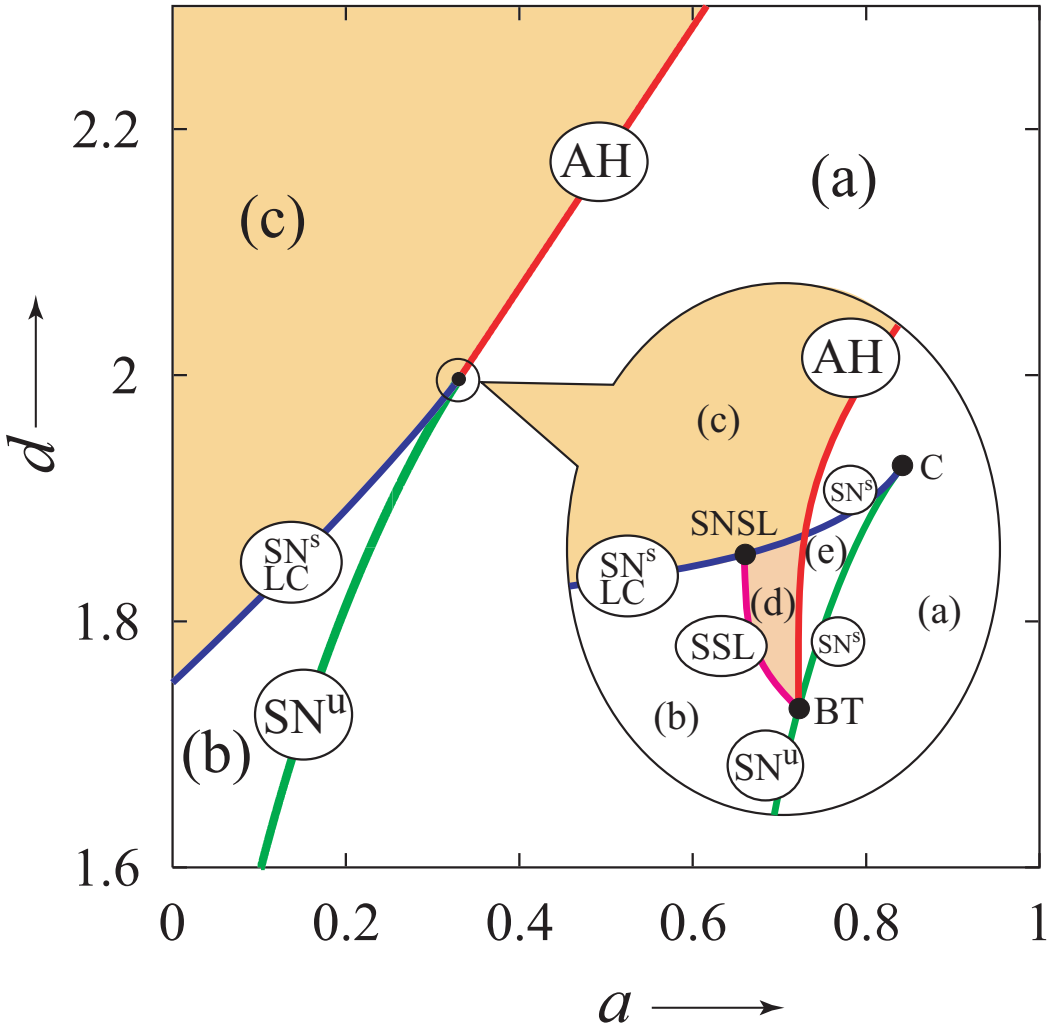

Figure 1: Bifurcation diagram of equilibria and limit cycles in Eqn. (3) for $b = 1$ and $c = 3$. AH: the (supercritical) Andronov-Hopf bifurcation, SN^sLC: a saddle-node on limit cycle bifurcation for a stable node and a saddle, SN^s (or, SN^u): a saddle-node bifurcation for a saddle and a stable node (or an unstable node), SSL: a saddle-separatrix loop bifurcation, BT: the Bogdanov-Takens bifurcation, C: a cusp, SNSL: a saddle-node on separatrix loop bifurcation. Phase planes in each region are shown in Fig. 2, and a stable limit cycle exists in the region (c) and (d).

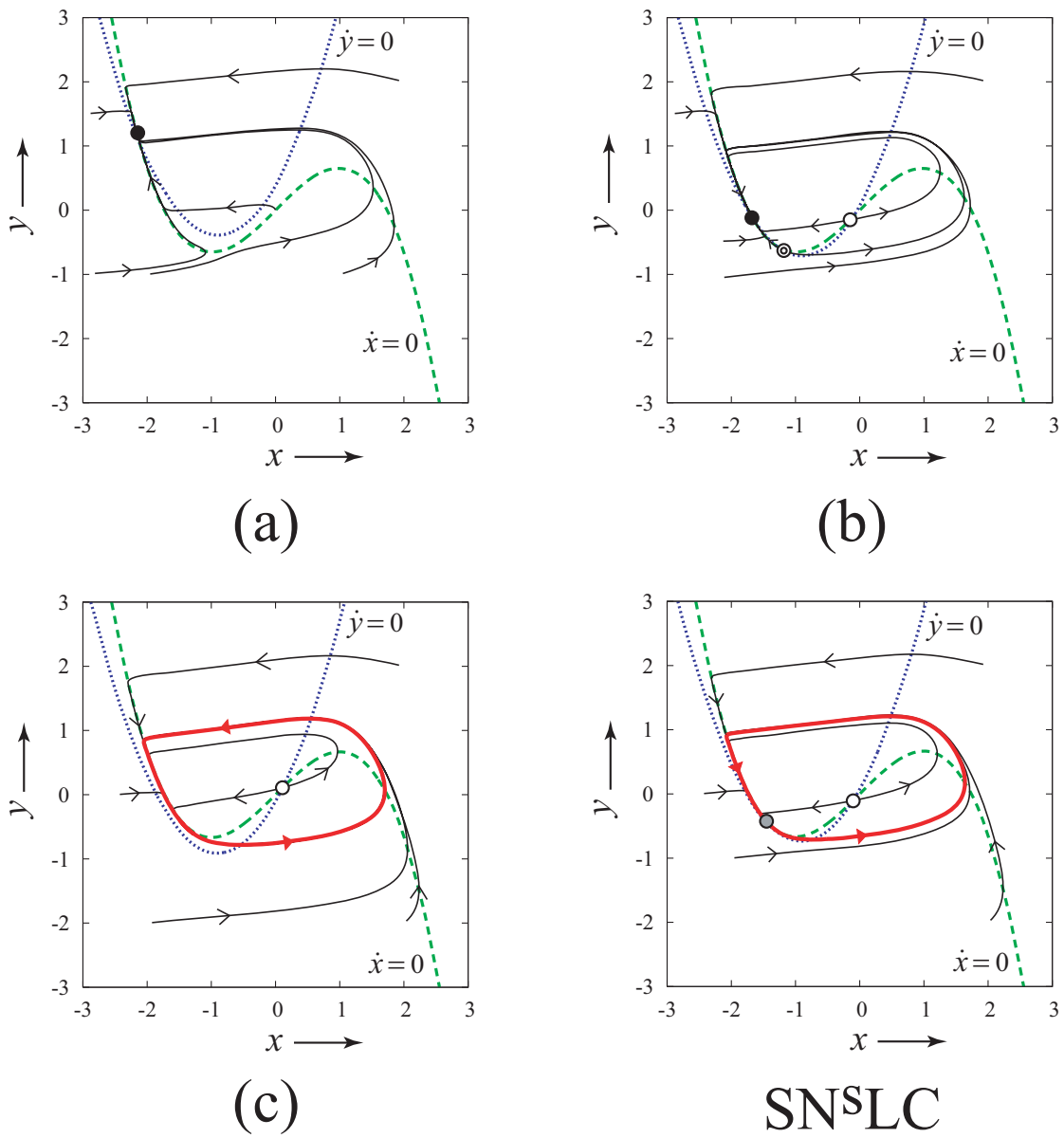

Figure 2: Phase portraits of the regions in Fig. 1. In these figures, black, white, and double circles represent stable, unstable, and saddle equilibrium points, respectively. Gray circle denotes a bifurcating point. Arrows indicate directions of trajectories, and red closed curve denotes a stable limit cycle.

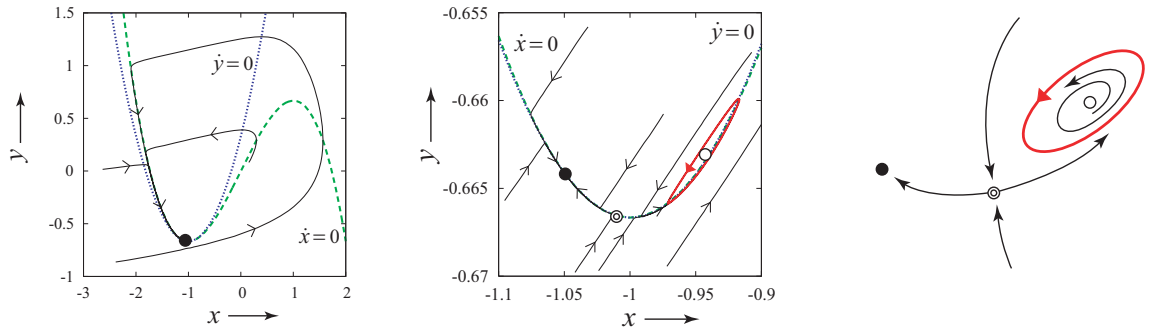

(d)

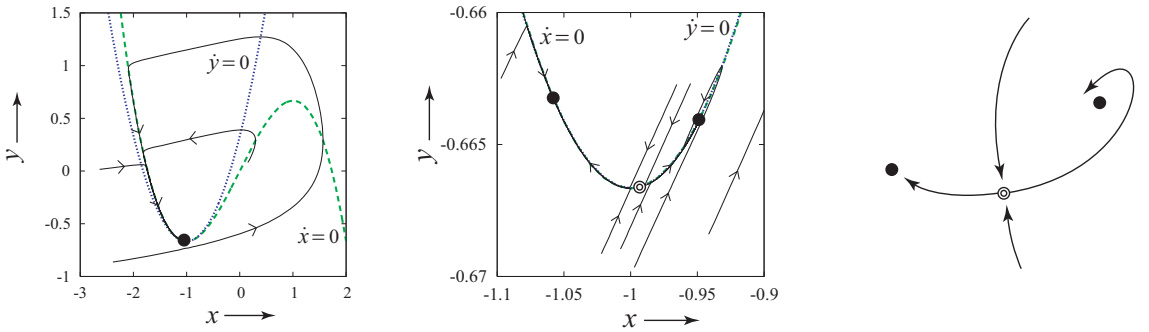

(e)

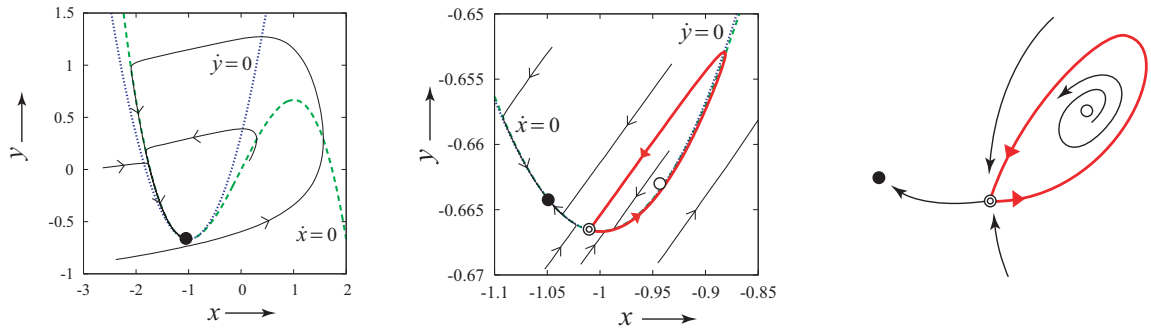

SSL

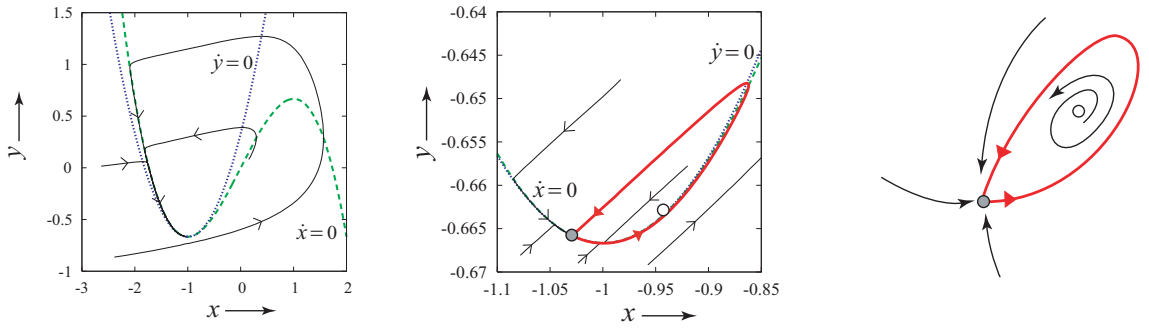

SNSL

Figure 2: *Continued.*

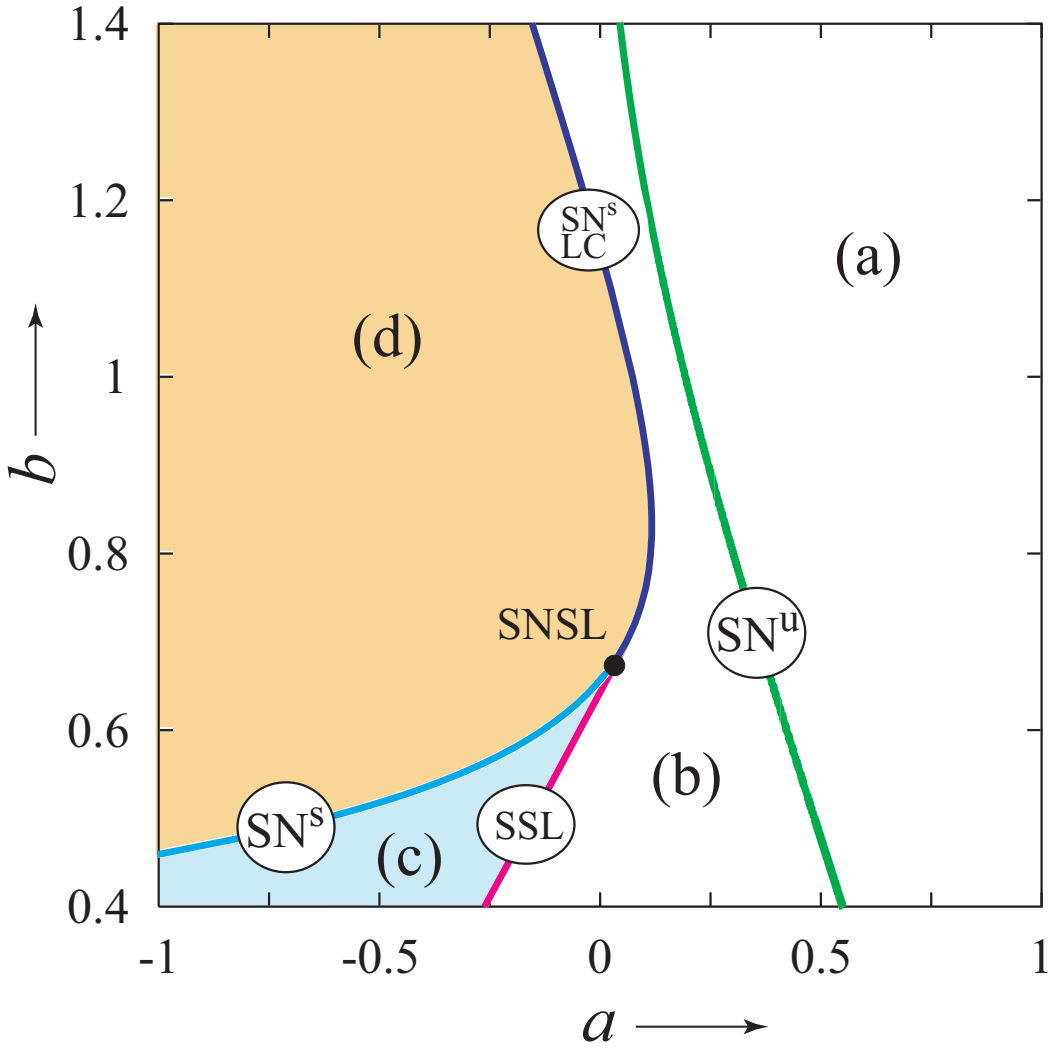

Figure 3: Bifurcation diagram of equilibria and limit cycles in the a-b parameter plane with $c = 3$ and $d = 1.8$. $\mathrm{SN^sLC}$: a saddle-node on limit cycle bifurcation for a stable node and a saddle, $\mathrm{SN^s}$ (or, $\mathrm{SN^u}$): a saddle-node bifurcation for a saddle and a stable node (or an unstable node), SSL: a saddle-separatrix loop bifurcation. There exists a stable limit cycle In region (c) and (d), while a stable equilibrium exists in the region (c). Phase planes in each region are shown in Fig. 4.

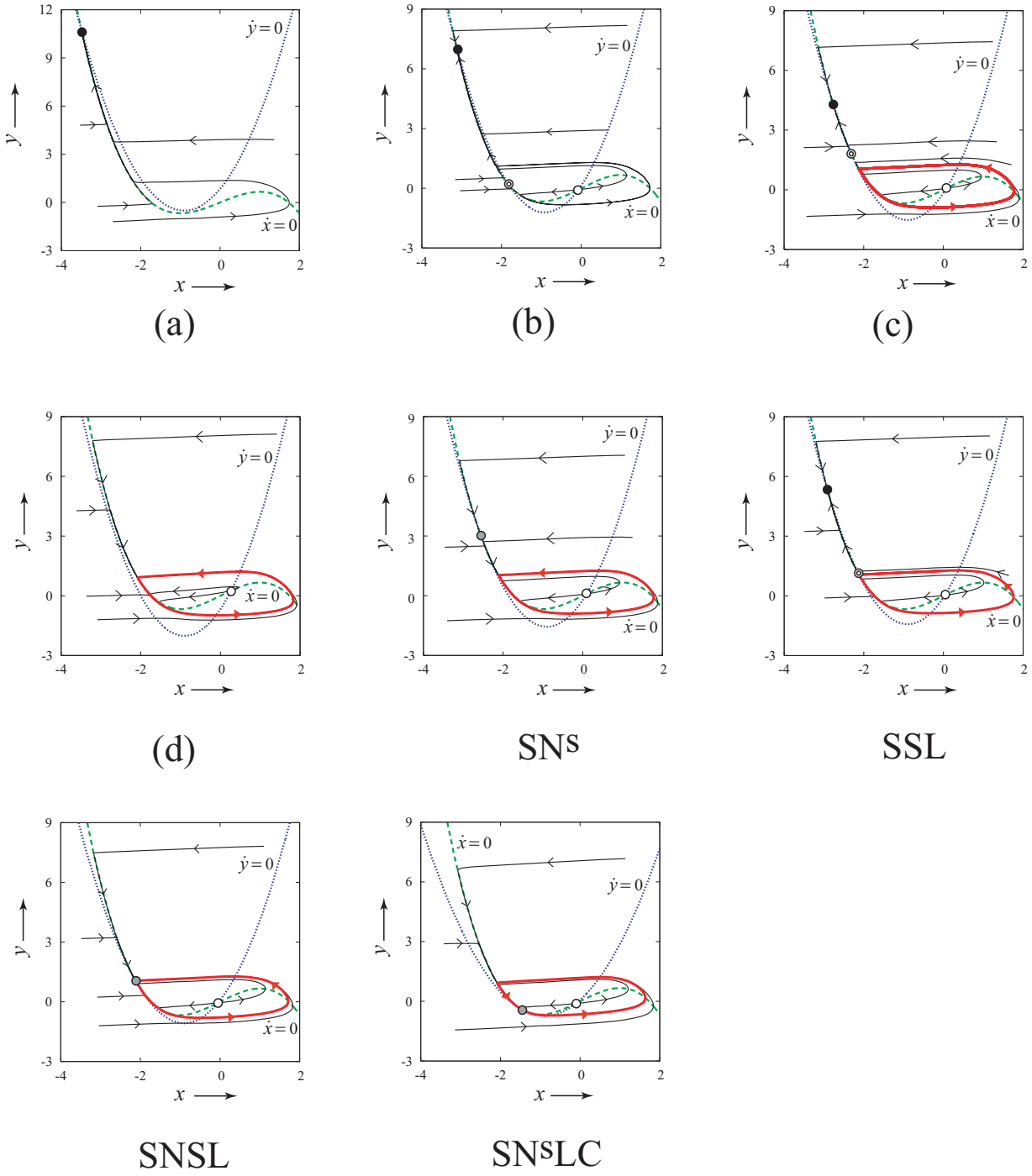

Figure 4: Phase portraits of the regions in Fig. 3.

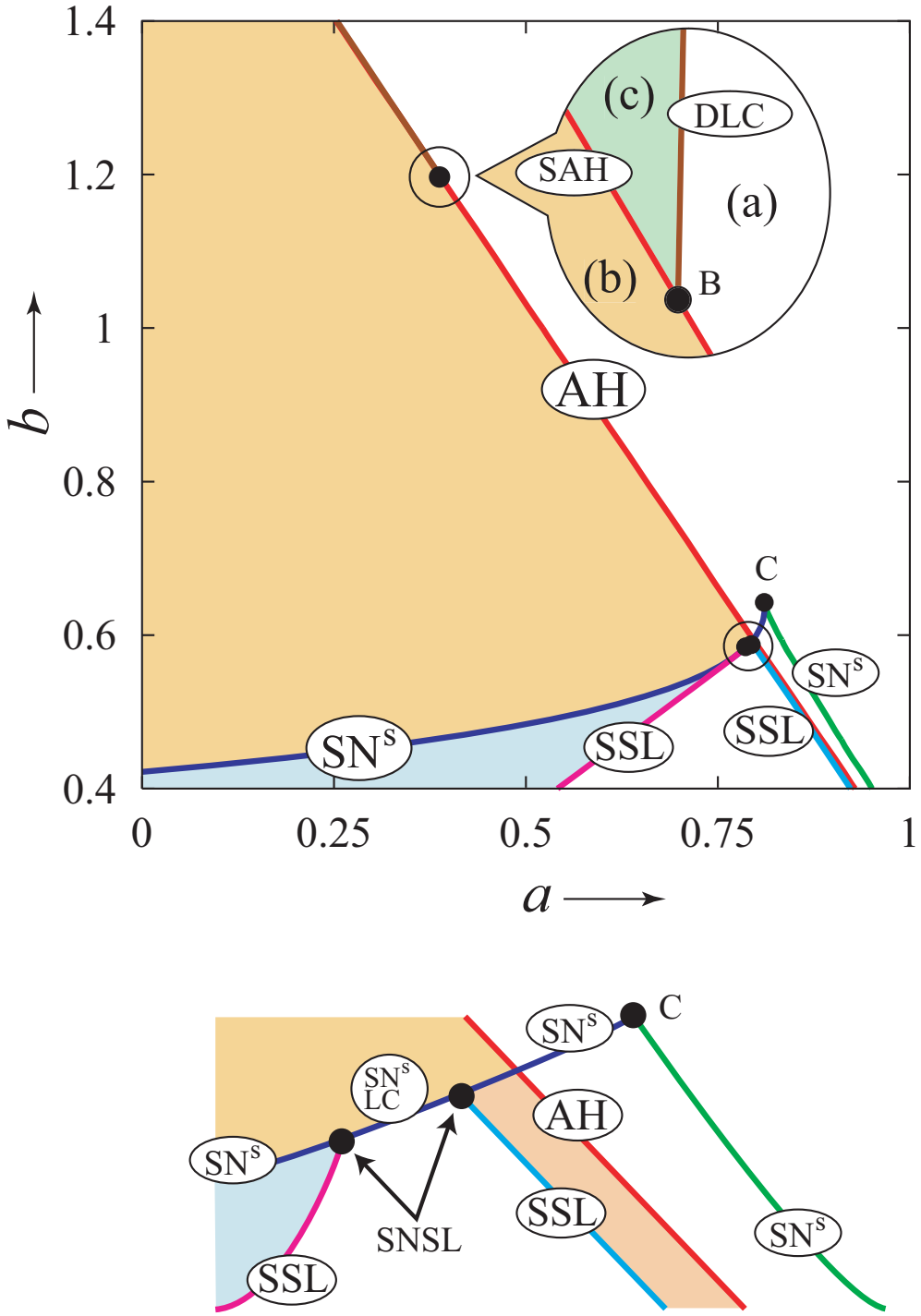

Figure 5: Bifurcation diagram of equilibria and limit cycles in the a-b parameter plane with $c = 3$ and $d = 2.2$ (*Upper*), and a enlarged schematic diagram around $a = 0.79$ and $b = 0.59$ in the upper figure (*Lower*). AH: the (supercritical) Andronov-Hopf bifurcation, SAH: the (subcritical) Andronov-Hopf bifurcation, SSL: a saddle-separatrix loop bifurcation, $\mathrm{SN^S}$: a saddle-node bifurcation for a saddle and a stable node, DLC: a double limit cycle bifurcation, $\mathrm{SN^S LC}$: a saddle-node on limit cycle bifurcation for a stable node and a saddle, C: a cusp, SNSL: a saddle-node on separatrix loop bifurcation. Phase planes in the regions (a), (b), and (c) are shown in Fig. 6. If we use parameter sets in the upper region, the system exhibits Class 2 excitability and Class 2 spiking with the bistability. On the other hand, the system exhibits Class 2 excitability and Class 1 spiking with the bistability if we choice parameter sets in the lower region.

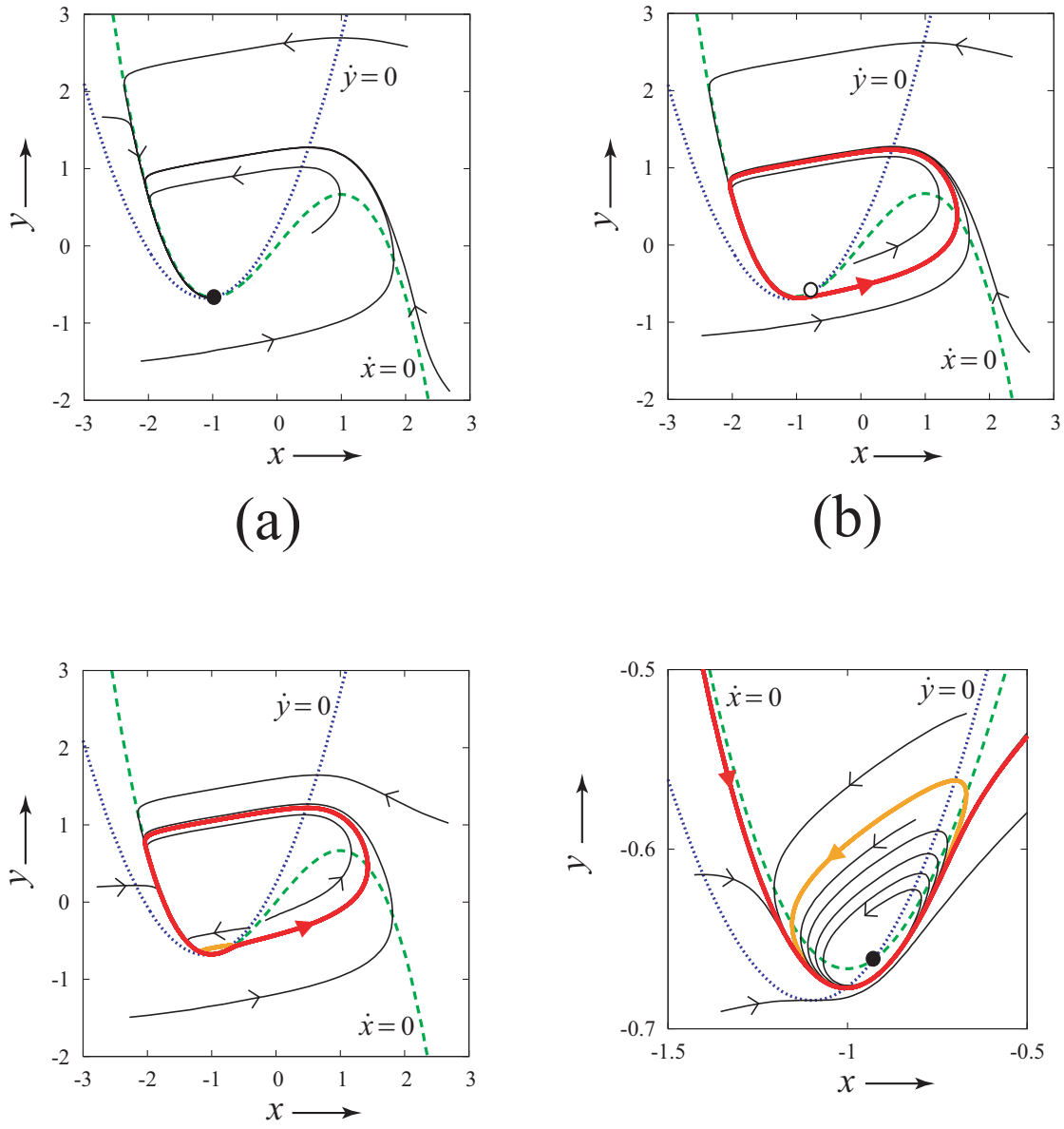

Figure 6: Phase portraits of some regions in Fig. 5. An orange closed curve denotes an unstable limit cycle.

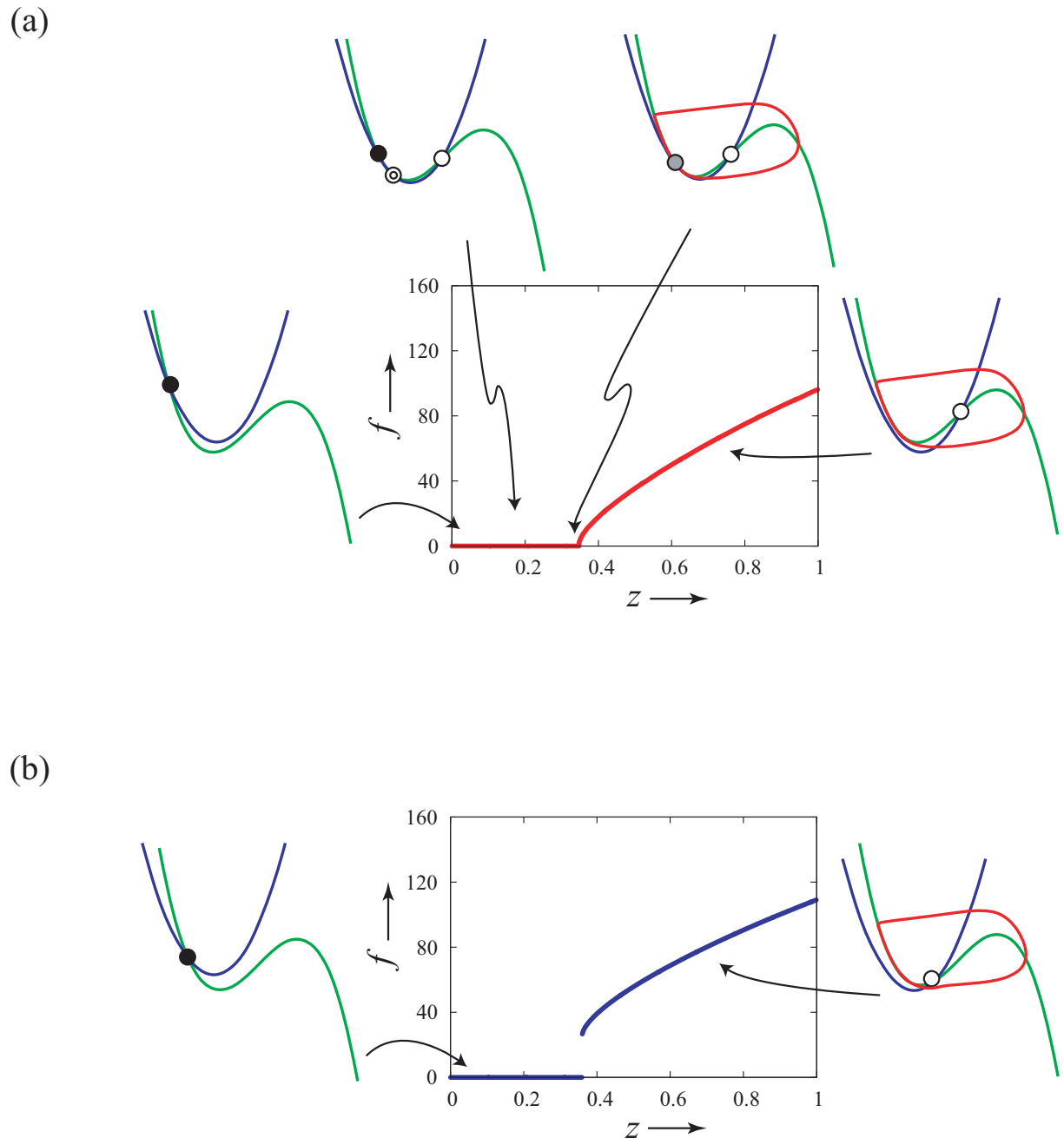

Figure 7: Firing frequency f depending on the intensity z of the input current. Parameter values in each figure are determined based on Figs. 1, 3, and 5 as follows: (a) $a = 0.42$, $b = 1$, $c = 3$, and $d = 1.8$, (b) $a = 0.88$, $b = 1$, $c = 3$, and $d = 2.2$, (c) $a = 0.08$, $b = 0.6$, $c = 3$, and $d = 1.8$, and (d) $a = 0.775$, $b = 1.3$, $c = 3$, and $d = 2.2$. Systems (a)-(d) exhibit "Class 1 excitability and Class 1 spiking", "Class 2 excitability and Class 2 spiking without the bistability", "Class 2 excitability and Class 1 spiking", and "Class 2 excitability and Class 2 spiking with the bistability", respectively.

(c)

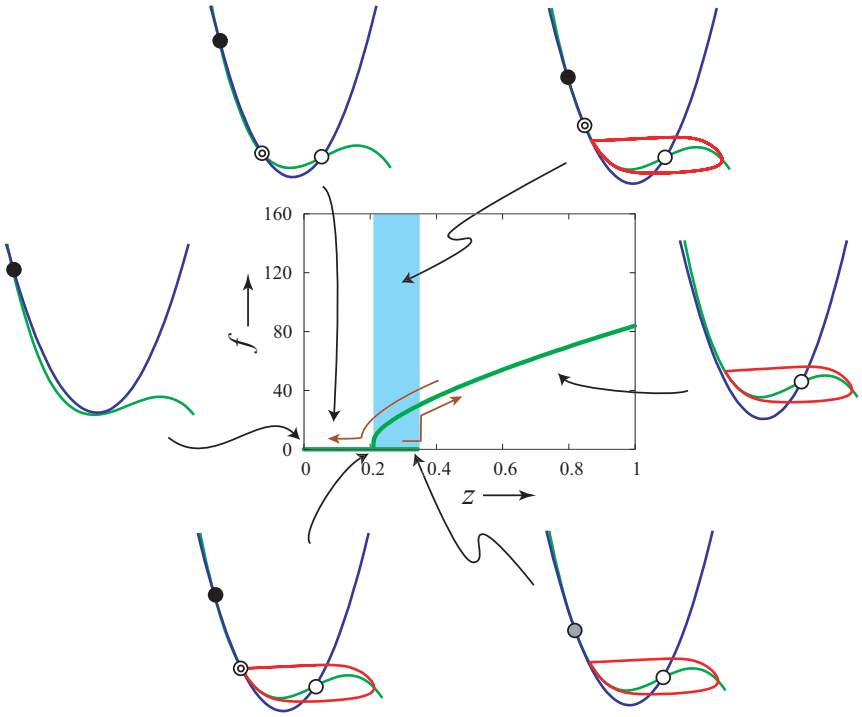

(d)

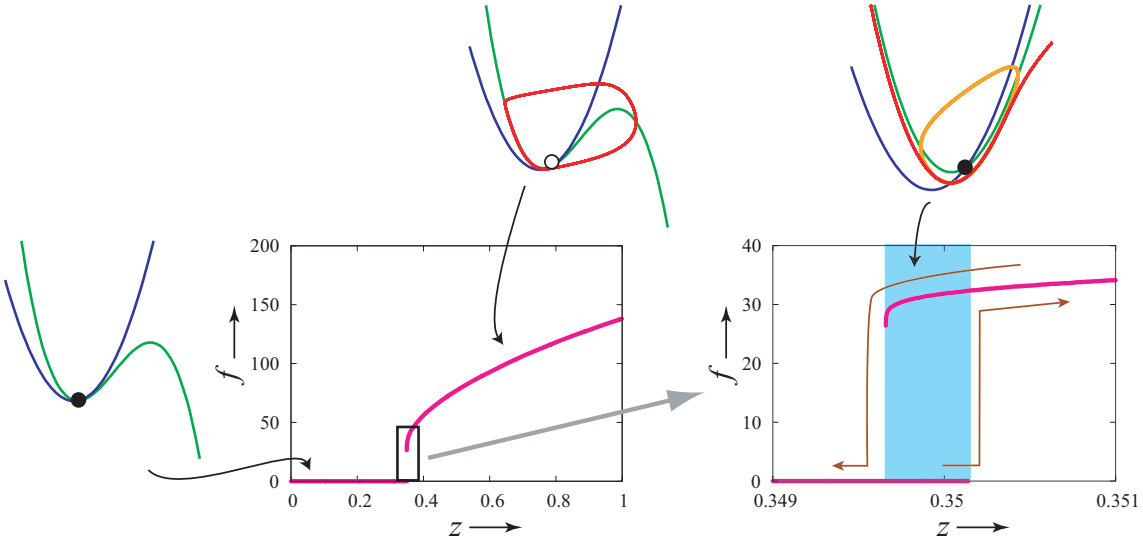

Figure 8: *Continued.*